UV/NIR-Light Triggered Rapid and Reversible Color Switching for Rewritable Smart Fabrics

8 authors, including:

Daniel K. Macharia
Donghua University
25 PUBLICATIONS   **333** CITATIONS

SEE PROFILE

Sharjeel Ahmed
Curtin University
4 PUBLICATIONS   **25** CITATIONS

SEE PROFILE

Zhaojie Wang
Yunnan University
45 PUBLICATIONS   **604** CITATIONS

SEE PROFILE

Josphat Igadwa Mwasiagi
Moi University
73 PUBLICATIONS   **303** CITATIONS

SEE PROFILE

Some of the authors of this publication are also working on these related projects:

Optimization of Vertical Double-Diffused Metal-Oxide Semiconductor (VDMOS) Power Transistor Structure for Use in High Frequencies and Medical Devices View project

Design and Scheduling of Garment Assembly Line Using Simulation-Based Optimization View project

UV/NIR-Light-Triggered Rapid and Reversible Color Switching for Rewritable Smart Fabrics

Daniel K. Macharia,[†] Sharjeel Ahmed,[†] Bo Zhu,[†] Zixiao Liu,[†] Zhaojie Wang,[†] Josphat Igadwa Mwasiagi,[‡] Zhigang Chen,*,[†] and Meifang Zhu*,[†]

[†]State Key Laboratory for Modification of Chemical Fibers and Polymer Materials, International Joint Laboratory for Advanced Fiber and Low-Dimension Materials, College of Materials Science and Engineering, Donghua University, Shanghai 201620, P. R. China

[‡]School of Engineering, Moi University, P.O. Box 3900-30100, Eldoret, Kenya

S *Supporting Information*

ABSTRACT: Remote, rapid, and ink-free printing/erasure on fabrics has great potential to revolutionize specialized clothing in numerous applications including fashion/aesthetic and security fields, but the construction of such smart fabrics has not been realized due to underlying obstacles in obtaining suitable photoreversible color-switching systems (PCSS). To address this problem, we have prepared TiO_{2-x} nanorods as photocatalytic and photothermal component. With redox dyes as reversible color indicators and hydroxyethyl cellulose (HEC) as polymer matrix, TiO_{2-x}/dye/HEC-based PCSS is coated on poly(dimethylsiloxane)-treated cotton fabric. Under 365 nm light irradiation, discoloration occurs in 180 s, resulting from the efficient photocatalytic reduction of the dye. On the contrary, when the colorless fabric is irradiated by 808 nm light, recoloration occurs in a very short time (∼100 s), far lower than the traditional heating mode (30−8 min at 90−150 °C). This rapid recoloration should be attributed to the localized high temperature (164.3−184.5 °C) induced by photothermal effect of TiO_{2-x}. Particularly, when TiO_{2-x}/dye/HEC-based PCSS is extended to coat commercial clothes (such as T-shirts), red/green/blue figures/letters can be rapidly and remotely printed by UV-light pen and then erased by near-infrared light, with high cycle stability. Therefore, such rewritable smart fabric represents an attractive alternative to regular clothes in meeting the increasing aesthetic or camouflage needs.

KEYWORDS: smart fabrics, TiO_{2-x} photocatalyst, color switching, UV-light printing, NIR-light erasing
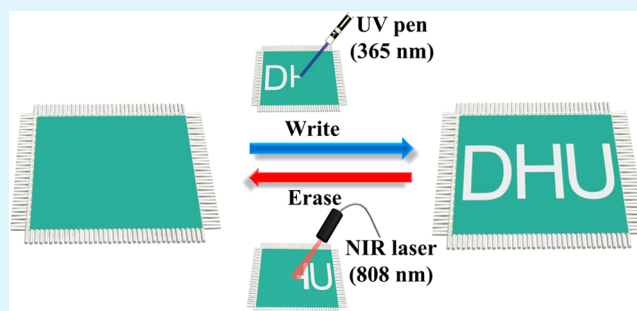
1. INTRODUCTION

Smart materials, whose chromatic transitions emanates from a selective response to external stimuli (such as heat, light, mechanical stress, etc.), have been attracting considerable attention, since they offer an exciting array of applications including sensors, displays, and switches.[1−5] In particular, photochromic materials are rather appealing, since light can be spatiotemporally manipulated to reversibly activate changes in the molecular structure of chromophores, thus switching their color.[6,7] Typically, photochromic materials have two different kinds of photochromism. One is "P" type photochromism in which reverse transition in molecular structures occurs photochemically, and typical materials include azobenzene photoswitches,[8,9] spiropyran,[10] and diarylethene derivatives.[5] However, these P type materials have some limitations, including low efficiency, few life cycles, and competing thermal back relaxation issues. The other is "T" type photochromism, which requires thermal-activated reverse transition of color. The T type materials include azobenzenes,[11] dyads,[12] donor−acceptor Stenhouse adduct photoswitches,[13,14] and photo-

reversible color-switching systems (PCSS).[15−19] Among these T type photochromic materials, PCSS have drawn increasing interest as new smart color-switching systems, and they are usually composed of semiconductor nanomaterials as photocatalytic agents, commercial redox dyes as reversible color indicators, and polymers as matrix. Several PCSS have been well developed for the color switching of solution/paper/film, such as TiO_2/dye/hydroxyethyl cellulose (HEC)[15−19] and SnO_{2-x}/dye/H_2O.[20] For example, TiO_2/methylene blue (MB)/HEC-based PCSS have been used for constructing the first ink-free light-printable rewritable paper.[15] Under the irradiation of UV−visible light, semiconductor nanomaterials in PCSS produce electron−hole pairs. Then, the photogenerated holes are captured by the sacrificial electron donors (SEDs), whereas the remaining electrons rapidly reduce the dyes to their leuco form usually in 10−150 s for solution[16,20,21]

and in 30 s to 10 min for film/paper.[15,17,22,23] Furthermore, the recoloration process for film/paper is majorly governed by the oxidation of the leuco dye back to its colored state under ambient air conditions for 12 h to 6 days or at 90−150 °C for 30−8 min.[15−17,20] It should be pointed out that the recoloration process is too slow for their future practical applications (such as wearable devices, adaptive camouflage). Although the uniform heating of PCSS-based film/paper at higher temperatures may result in short recoloration time, it will have some obvious adverse effects. For example, when the rewritable paper was heated at 115 °C during recoloration process, it turned from blue to slightly yellowish.[15] Therefore, it is imperative to develop novel PCSS with short recoloration time and no adverse effects.

Recently, smart fabrics have drawn great interests in the world on the account of having additional functions and doing many things that traditional fabrics cannot. Smart fabrics can be divided into two kinds: aesthetic (such as color-tunable fabrics[24,25] and photonic fabrics[26]) and performance enhancing (such as wearable electronic textiles,[27,28] self-cleaning textiles,[29] and e-skin[30,31]). Among these aesthetic smart fabrics, the fabrics with color-switching properties are very attractive due to their fascinating features that enable applications in specialized clothing for sensors, information displays, fashion/aesthetic, and security fields. Several photochromic fabrics have been prepared such as SiO$_2$-naphthopyran fabrics[32] and color dosimeter fabrics.[33] Nevertheless, they suffer from some drawbacks, including rough texture of fabrics, photoinstability, low sensitivity, and lack printing/erasing features. Ideally, the color and figures on smart fabrics should be controlled remotely and rapidly. Therefore, there still remains a great challenge to develop new smart fabrics with remote and rapid color-switching features.

Near-infrared (NIR)-light responsive photothermal nano-materials have been widely used in smart windows,[34] mechanical oscillators,[35] microfluidic heating,[36] and cancer therapy.[37,38] Our group has also developed several photo-thermal nanoagents (such as CuS,[39,40] W$_{18}$O$_{49}$,[41] and Nb-doped TiO$_2$[42]) for the ablation therapy of tumor. Under the irradiation of NIR laser (808/915/980/1064 nm), photo-thermal nanomaterials can absorb the NIR light and convert it to heat, resulting in the localized high temperature (such as 80−140 °C for carbon nanotubes-containing poly-(dimethylsiloxane) (PDMS) elastomer,[43] and nanosilver conducting ink[44]). In fact, the localized high temperature can be remotely controlled by adjusting the intensity of NIR light. This localized high temperature inspired our interest in the novel concept of developing PCSS-based smart fabric with rapid response. Herein, with Ti^{3+} self-doped TiO$_{2−x}$ nanorods as the model of photocatalytic and photothermal component, redox dyes (methylene blue (MB), neutral red (NR), and acid green 25 (AG)) as reversible color indicators, and hydrox-yethyl cellulose (HEC) as natural polymer matrix, we developed a TiO$_{2−x}$/dye/HEC PCSS solution with rapid discoloration/recoloration abilities driven by UV/NIR light. The PCSS solutions were used to construct smart photo-chromic fabrics. Letters/figures on the surface of smart fabrics were remotely printed by UV-light pen and then erased by NIR light with high resolution and excellent cycling stability.

2. EXPERIMENTAL SECTION

2.1. Materials. Titanium fluoride (TiF$_4$), titanium(III) chloride (TiCl$_3$), poly(ethylene glycol) (PEG-400), ethylene glycol (EG),

slygard 184 silicon elastomer (poly(dimethylsiloxane), PDMS), tetrahydrofuran (THF), hydroxyethyl cellulose (HEC), methylene blue (MB), neutral red (NR), and acid green 25 (AG) were all obtained from Sigma-Aldrich and used as received without further purification.

2.2. Synthesis and Color Switching of PCSS Solution. TiO$_{2−x}$ nanorods were synthesized by a modified solvothermal method.[45] In a typical process, TiF$_4$ powder (0.124 g, 1 mmol) was added into ethanol (12.5 mL) and the solution was stirred for 20 min to form a uniform pale yellow solution. Then, TiCl$_3$ liquid (2.5 mL, 42.8 mmol) and PEG-400 (12.5 mL) were rapidly added into the above solution, and the resulting solution was continuously stirred for 15 min to obtain a purple suspension. The resultant suspension was transferred into a Teflon-lined autoclave (30 mL) and heated at 180 °C for 20 h. Blue Ti^{3+} self-doped TiO$_{2−x}$ precipitates were obtained by centrifuging the colloidal suspension. The precipitates were then thoroughly washed in alcohol three times. A portion of TiO$_{2−x}$ precipitates was dissolved in the distilled water to obtain the solution with a required concentration (10 mg mL$^{−1}$), and the other portion was dried at 60 °C for 10 h for further analysis. The characterization of the samples was shown in the Supporting Information.

To investigate the color switching in solution, PCSS solution with low concentration was prepared by mixing aqueous solution (1 mL) of TiO$_{2−x}$ nanorods (10 mg mL$^{−1}$), aqueous solution (25 μL) of redox dye (MB, 0.01 M), and the distilled water (20 mL). The PCSS solution was then transferred into a glass cuvette (2 mL), degassed for 20 min under N$_2$ gas, and then tightly sealed. To discolor, the PCSS solution was irradiated by a UV light (365 nm, 250W Hg lamp, Philips Lighting Luminaires Co. Ltd., Shanghai, China). To recolor, the tightly sealed glass cuvette was opened to expose it to air and irradiated by 808 nm laser (∼1.0 W cm$^{−2}$). The absorption spectra of PCSS solution were recorded during the discoloration and recoloration process by UV−vis−NIR spectrophotometer (Shimadzu UV-3600).

2.3. Construction and Color Switching of Smart Fabrics. For constructing the smart photochromic fabrics, PCSS inks with high dye concentration were prepared by homogeneously mixing aqueous solution (4 mL) of TiO$_{2−x}$ nanorods (10 mg mL$^{−1}$), HEC aqueous solution (4 mL, 33.33 mg mL$^{−1}$), an aqueous solution (0.8 mL) of redox dye (MB/NR/AG, 0.01 M), and EG (1 mL) under magnetic stirring for 15 min. Then, flexible cotton fabrics were tailored to have the sizes of 6 × 6 cm^2 and immersed in an aqueous solution (100 mL) containing H$_2$O$_2$ (4 mL), NaOH (3 g), and MgSO$_4$ (3 g). The solution with the fabrics was heated at 100 °C for 1 h to remove impurities such as waxes and pectins. After that, cotton fabrics were taken out, washed thoroughly with distilled water, and then dried at 60 °C for 30 min. To fill up the texture pores and obtain the hydrophobicity, cotton fabrics were coated with PDMS-based THF solution (the mixture of 30 mL THF, 10 mL PDMS, and 1.5 mL curing agent) by using doctor blade method and dried at 80 °C for 12 h to obtain a uniform PDMS layer on both surfaces of fabrics. At last, with PDMS-coated cotton fabrics as the substrate, PCSS inks were coated on the surface by doctor blade method, and the resulting fabrics were dried at 60 °C for 12 h, forming flexible, smooth, and colored smart fabrics. For evaluating the possible practical application, the central portions of commercial T-shirts were also coated successively with PDMS-based THF solution and PCSS inks under other identical conditions.

To investigate the color switching of smart fabrics, the fabrics were irradiated with UV-light pen (365 nm, ∼4 W cm$^{−2}$) to discolor the redox dyes and then the reverse color transition was attained by the irradiation of 808 nm light (∼1.0 W cm$^{−2}$). To print images on the smart fabrics, photomasks with various designs should be used. To investigate the photothermal effects, the smart fabrics were irradiated with 808 nm light and then their temperature was real-time recorded by using an infrared camera (FLIR-A300, FLIR Systems Inc.). The microsurface temperature distribution of the fabric was captured by an infrared camera fitted with a microlens.

3. RESULTS AND DISCUSSION

Ti^{3+} self-doped TiO_{2-x} nanorods were prepared by a simple solvothermal route with TiF_4 and $TiCl_3$ as Ti precursors, PEG-400 as the surface ligand, and ethanol as the solvent. For comparison, the undoped TiO_2 nanorods were obtained by using TiF_4 as the only Ti precursor under other identical conditions. The sizes and morphologies of both TiO_{2-x} and TiO_2 samples were investigated by transmission electron microscopy (TEM). Obviously, TiO_{2-x} sample is composed of uniform nanorods with diameters of ~16 nm and lengths of ~33 nm (Figure 1A). High-resolution transmission electron
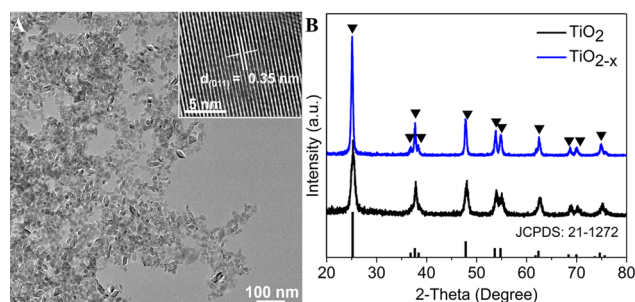
Figure 1. (A) TEM image of TiO_{2-x} sample and (B) XRD patterns of TiO_2 and TiO_{2-x} samples.

microscopy image (the inset in Figure 1A) indicates clear lattice fringes, suggesting that TiO_{2-x} nanorod is a single crystal. The interplanar d-spacing is determined to be 0.35 nm, which corresponds well with the (101) planes of tetragonal anatase TiO_2 (JCPDS no. 21-1272). Similarly, the TiO_2 sample consists also of uniform nanorods with diameters of ~16 nm and lengths of ~33 nm (Figure S1). In addition, the phases of both TiO_{2-x} and TiO_2 nanorods were studied by X-ray diffraction (XRD) pattern. Both samples exhibit similar diffraction peaks, and all these diffraction peaks can be well indexed to the tetragonal anatase TiO_2 (JCPDS no. 21-1272) without any impurities (Figure 1B). With TiO_{2-x} sample as the model, the energy-dispersive X-ray spectroscopy (EDS) pattern reveals that besides Cu signal from copper grid, TiO_{2-x} sample is composed of Ti and O elements (Figure S2A). Elemental maps (Figure S2B) in the scanning transmission electron microscopy mode reveal that Ti and O are homogeneously distributed among the nanorods. These results confirm the well formation of tetragonal anatase nanorods, and Ti^{3+} self-doping has no obvious effect on the morphology and phase.

To determine the presence of Ti^{3+} and oxygen vacancy in TiO_{2-x} sample, TiO_{2-x} and TiO_2 nanorods were investigated by Raman, X-ray photoelectron spectroscopy (XPS), and electron paramagnetic resonance (EPR) spectra. Raman spectroscopy reflects the vibration of molecular bonds with high measuring sensitivity, and it can be used to investigate significant structural changes from oxygen vacancies in titania.[46] Both TiO_{2-x} and TiO_2 nanorods show similar four Raman peaks at 197, 398, 515, and 639 cm^{-1} (Figure 2A), corresponding to the stretching modes of Ti–O bands in the anatase phase of TiO_2 crystal. The undoped TiO_2 nanorods show another strong Raman peak at 142.2, but this peak for TiO_{2-x} nanorods shifts to 146.4 cm^{-1} with obvious broadening. This shift and broadening should be assigned to the disorder in TiO_2 crystal due to the presence of Ti^{3+} species, which is similar to the previous report.[47] In addition, the XPS
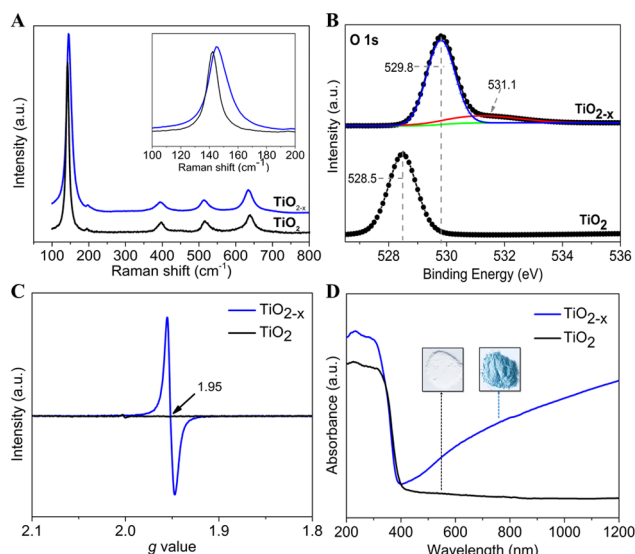
Figure 2. Raman spectra (A), O 1s XPS spectra (B), X-band EPR spectra (C), and UV–vis–NIR diffuse spectra (D) of TiO_{2-x} as well as TiO_2 nanorod samples.

analysis can be used to investigate the chemical states of Ti and O. High-resolution O 1s spectrum (Figure 2B) of TiO_2 nanorods reveals the presence of strong peak at 528.5 eV, which corresponds to lattice oxygen (Ti–O) of TiO_2.[48] However, O 1s spectrum of TiO_{2-x} nanorods indicates that the predominant peak is located at 529.8 eV with a positive shift of ~1.3 eV. The previous report has revealed that O 1s binding energy/peak of TiO_2 oxidized by H_2O_2 was shifted to lower energy/intensity compared to that of original TiO_2, resulting from larger numbers of O atom than Ti atom numbers in TiO_2.[48] In our case, O 1s positive shift (~1.3 eV) from TiO_{2-x} nanorods should be attributed to the fact that the number of O atoms in TiO_{2-x} were lesser than the number of Ti atoms, suggesting the presence of oxygen vacancies. A new but weak peak at 531.1 eV can be found for TiO_{2-x} nanorods, and it can be attributed to the surface hydroxyl groups (Ti–OH) (Figure 2B).[49,50] In addition, Ti 2p spectra of both TiO_2 and TiO_{2-x} samples show two similar peaks at 458.3 and 464.0 eV, which can be well assigned to the Ti^{4+} oxidation state (Figure S3). The TiO_{2-x} sample has no additional peaks for Ti^{3+} species, which should appear at about 457.9 eV for Ti^{3+} $2p_{1/2}$ and 463.6 eV for Ti^{3+} $2p_{3/2}$. This fact reveals that the surface of TiO_{2-x} nanorods should be TiO_2, which suggest the formation of TiO_2 nanoshell on TiO_{2-x} cores for TiO_{2-x} samples and is similar to the previous report.[45] Furthermore, EPR spectroscopy is an excellent method for studying materials with unpaired electrons, and it has been well used to confirm the presence of Ti^{3+} in Ti^{3+} self-doped TiO_{2-x} nanorods.[42,45,49−53] Before doping, the TiO_2 sample does not show any paramagnetic signal (Figure 2C). On the contrary, the TiO_{2-x} sample shows strong g values at ~1.95, which should result from the paramagnetic Ti^{3+} species and suggests the formation of Ti^{3+} centers in TiO_{2-x} crystal lattice.[42,45,52,53] Usually, the presence of Ti^{3+} centers are accompanied by the formation of oxygen vacancies. Notably, no EPR signal at 2.005 can be found for oxygen vacancies, which suggests the absence of Ti^{3+} centers on the surface.[42,45,52,53] Thus, one can deduce that Ti^{3+} centers should exist in the bulk rather than on the surface of TiO_{2-x} nanorods. Based on all above results, one can confirm the well formation of Ti^{3+} self-doped TiO_{2-x}
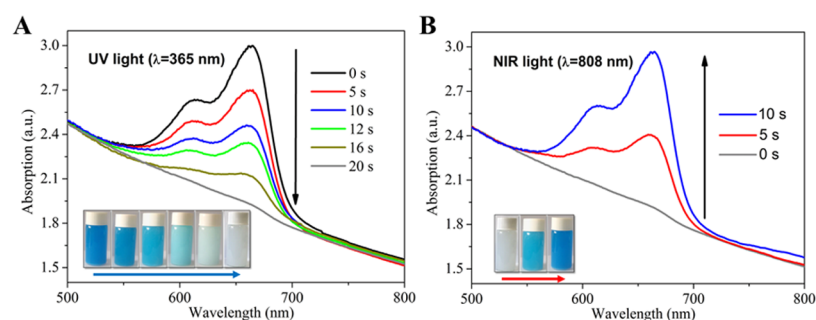
Figure 3. UV−vis−NIR spectra of TiO_{2-x}/dye/H_2O PCSS during (A) the discoloration process under UV irradiation for different times (0−20 s) and (B) the recoloration process under 808 nm irradiation for different times (0−10 s). The insets are the corresponding photos.
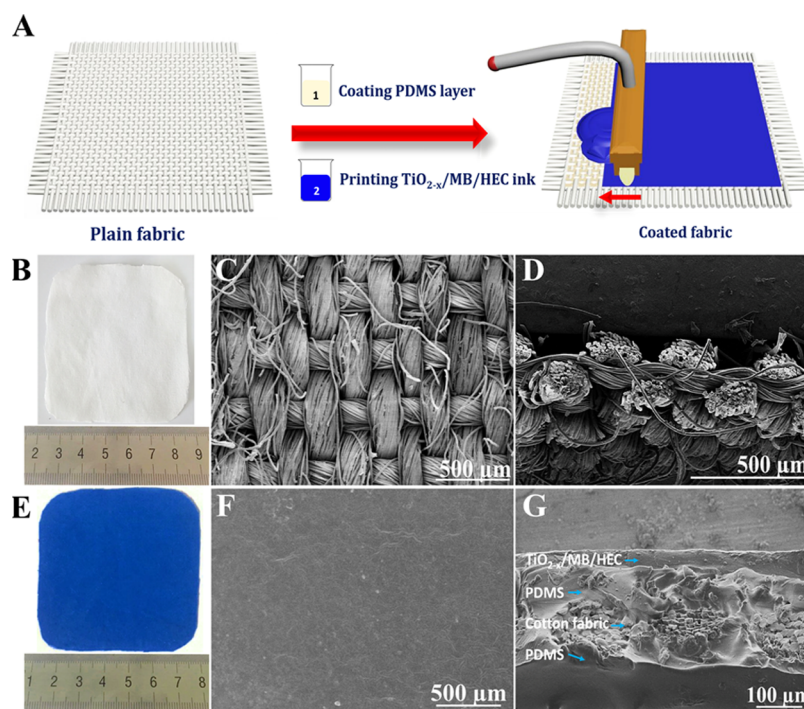
Figure 4. (A) Schematic illustration of the two-step coating process for PDMS and PCSS on cotton fabric. Photo (B), surface (C), and cross-sectional (D) SEM images of cotton fabric. Photo (E), surface (F), and cross-sectional (G) SEM images of smart fabric.

nanorods with TiO_2 layer as shell and oxygen vacancies in the bulk.

It is well known that doping has a strong effect on the optical properties of nanomaterials. To investigate the effect of doping on photoabsorption, both TiO_{2-x} and TiO_2 samples were measured by UV−vis−NIR diffusive reflectance spectrophotometer (Figure 2D). The undoped TiO_2 sample has white color and exhibits UV photoabsorption with an edge at ∼390 nm, which agrees well with the intrinsic wide band gap (∼3.2 eV). Interestingly, the TiO_{2-x} nanorods are blue. Besides a strong band gap photoabsorption, the TiO_{2-x} nanorods have a gradually enhanced photoabsorption with the increase of wavelength from ∼390 to 1200 nm. This enhanced photoabsorption in visible−NIR region should be attributed to strong localized plasmon resonance (LSPR), which originates from the presence of plenty of oxygen vacancies due to Ti^{3+} doping and is similar to the previous reports for TiO_{2-x} nanorods.[45,51,53]

Since TiO_{2-x} nanorods exhibit a strong UV and NIR photoabsorption, they can be used to prepare smart PCSS solution (TiO_{2-x}/dye/H_2O) with photoresponce. With MB as

a model of redox dye, the color switching of TiO_{2-x}/MB/H_2O solution was investigated under the irradiation of 365 or 808 nm light (Figure 3). Before the irradiation, TiO_{2-x}/MB/H_2O solution is blue and displays two clear peaks at 609 and 668 nm, which is consistent with the absorption peaks of MB. When UV light (365 nm, 4 W cm^{-2}) is first used to irradiate TiO_{2-x}/MB/H_2O solution, the blue color of the solution is gradually faded and then completely disappears in a short time of 20 s (the inset in Figure 3A). To further investigate the color evolution, the absorption spectrum of the solution was recorded by UV−vis−NIR spectrophotometer (Figure 3A). With the increase in UV-irradiation time from 0 to 20 s, both two peaks at 609 and 668 nm decrease and finally vanish, suggesting the efficient discoloration process by UV light. On the contrary, when 808 nm light is used to irradiate the leuco solution, its color reverts rapidly to its original blue hue and its absorption spectrum also recovers completely in 10 s (Figure 3B), indicating the rapid recoloration process by NIR light. During these discoloration and recoloration processes, the solution is very clear and no precipitates can be found.

Therefore, the present PCSS solution (TiO$_{2-x}$/dye/H$_2$O) has excellent color-switching features.

In the previous reports, the color-switching features of PCSS solutions confer their great potential in the application for rewritable papers.[16,17,19,20] In fact, if clothes possess color-switching features, they can be used as novel smart fabrics and can be very interesting/important applications for sensors, information displays, fashion/aesthetic, and security fields. To fabricate such smart fabrics, TiO$_{2-x}$/MB/HEC ink was prepared by coupling TiO$_{2-x}$ dispersion, redox dye (MB as a model), and hydroxyethyl cellulose (HEC), where HEC is a polymer matrix that aids in the formation of a coating layer on the treated fabric. Smart fabric was prepared by a two-step doctor blade method with cotton fabric as the substrate and TiO$_{2-x}$/MB/HEC as ink (Figure 4A). Before the coating, the cotton fabric is white (Figure 4B). The scanning electron microscopy (SEM) image (Figure 4C) shows that the pristine cotton fabric is composed of an interwoven fibrous structure containing fiber bunches with uniform diameters of ~200 μm. The cross-sectional SEM image shows that the fabric has bundles of fiber ends in the woven structure (Figure 4D). As we know, cotton is a porous and very absorbent material, and therefore in our case, dye molecules may easily be absorbed into the fiber pores, which would cause an irreversible color-switching effect. To avoid this irreversible behavior, the PDMS layer was first coated on both surfaces of clean cotton fabric (Figure 4A). The PDMS-coated cotton fabric exhibits a smooth surface, and the interwoven fibrous structure cannot be observed (Figure S4A). Cross-sectional SEM image (inset of Figure S4B) further confirms the well encapsulation of fibers by PDMS coating, which confers excellent hydrophobicity (Figure S4B−D), restricting the permeation of water/dye into the fabric. The second step is to prepare PCSS layer on PDMS-coated fabric with TiO$_{2-x}$/MB/HEC ink (Figure 4A). The color of smart fabric turned from white to complete blue, which is consistent with the MB color (Figure 4E). The surface SEM image (Figure 4F) reveals that the smart fabric has a smoother surface, and no protruding fibers can be found. Cross-sectional SEM image (Figure 4G) indicates that the interwoven fiber-bundle layer is well encapsulated by PDMS layer, and the surface of PDMS layer is coated with a TiO$_{2-x}$/MB/HEC layer with a uniform a thickness of ~50 μm. It should be noted that TiO$_{2-x}$/MB/HEC layer does not have direct contact with the fiber-bundle layer, avoiding the adverse effects of the pore structure of cotton fabric but favoring the color switching on the surface of smart fabric.

To realize the color-switching, smart fabric was discolored by UV light (365 nm, ~4.0 W cm^{-2}) irradiation and then recolored by NIR light (808 nm, ~1.0 W cm^{-2}) irradiation. Obviously, after the irradiation of UV light, the blue color of the smart fabric progressively fades with the increase of irradiation time from 0 to 180 s (Figure 5A). Concurrently, two photoabsorption peaks of MB at 609 and 668 nm gradually goes down with the increased time, until it almost completely flattens in 180 s (Figure 5B). On the contrary, when the colorless fabric is irradiated by 808 nm light, the blue color rapidly appears from 0 to 60 s and finally the smart fabric exhibits its initial blue color at 100 s (Figure 5C). Simultaneously, the absorption spectrum of the smart fabric goes up rapidly with irradiation time, and it fully recovers to the original absorption level in 100 s (Figure 5D). The present recoloration time (100 s) is very short, far lower than that from traditional heating model, such as 8 min at 115 °C for TiO$_2$/
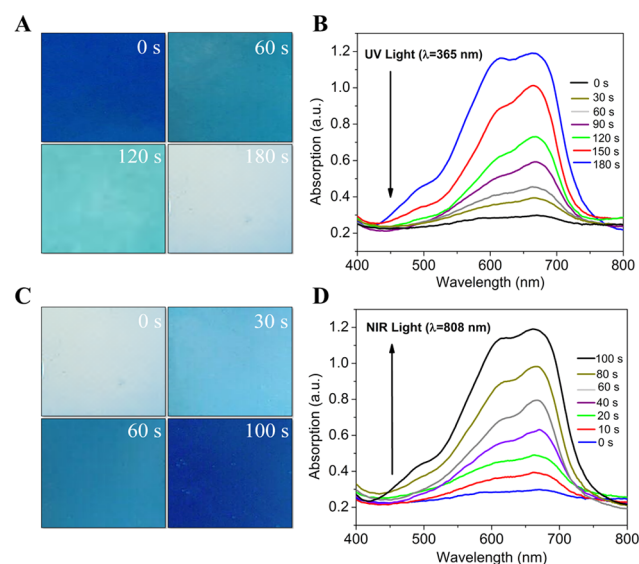
Figure 5. Photo (A) and UV−vis−NIR spectra (B) of smart fabric based on TiO$_{2-x}$/MB/HEC during the discoloration process under UV light irradiation for different times (0−180 s). The photo (C) and UV−vis−NIR spectra (D) of smart fabric during the recoloration process under NIR light irradiation for different times (0−100 s).

MB/HEC solid film,[15] 30 min at 120 °C for Ba-doped TiO$_2$/MB/HEC film.[16] Therefore, the smart fabric displays excellent and rapid discoloration process of PCSS solution by UV light, as well as rapid recoloration process by NIR light.

To reveal the rapid discoloration/recoloration mechanism by UV/NIR light, we investigated the effects of oxygen vacancies and O$_2$. When the undoped TiO$_2$ without oxygen vacancy is used to prepare TiO$_2$/MB/HEC layer on PDMS-coated fabric, the resulting fabric cannot show any blue discoloration and/or photoabsorption reduction (Figure S5A,B) under UV-light irradiation even after long duration (15 min). Since the blue color of smart fabric based on TiO$_{2-x}$/MB/HEC can be almost completely faded by UV-light irradiation in only 3 min, one can deduce that oxygen vacancies in TiO$_{2-x}$ acting as sacrificial electron donors are vital for rapid and efficient discoloration. In addition, to avoid the effect of O$_2$ in air, smart fabric based on TiO$_{2-x}$/MB/HEC was sealed in a plastic bag and air sucked out (Figure S6). This smart fabric was then irradiated by UV light, and the irradiated area showed rapid blue-fading, confirming that O$_2$ is not necessary for the discoloration process. When the colorless area of smart fabric is illuminated by NIR light, no apparent change could be observed even after 5 min, indicating that the recoloration process is inefficient in the absence of O$_2$. Therefore, one can confirm that both oxygen vacancies in TiO$_{2-x}$ and ambient O$_2$ are vital for the color switching of TiO$_{2-x}$/MB/HEC.

Subsequently, the effects of temperature were investigated for analyzing the rapid recoloration process of smart fabric based on TiO$_{2-x}$/MB/HEC. A colorless smart fabric was left in ambient conditions (in air, room temperature of 25 °C), and the exposure effect was quantified spectrophotemetrically. The absorption peaks reverted back slowly to the original intensity in ~10 h (Figure 6A). This slow recovery stems from the continued oxidation of LMB* to MB by O$_2$ under ambient laboratory conditions, which is similar to the previous reports.[15−17] Although oxygenation alone can result in the recoloration of the smart fabric, the process is very slow and
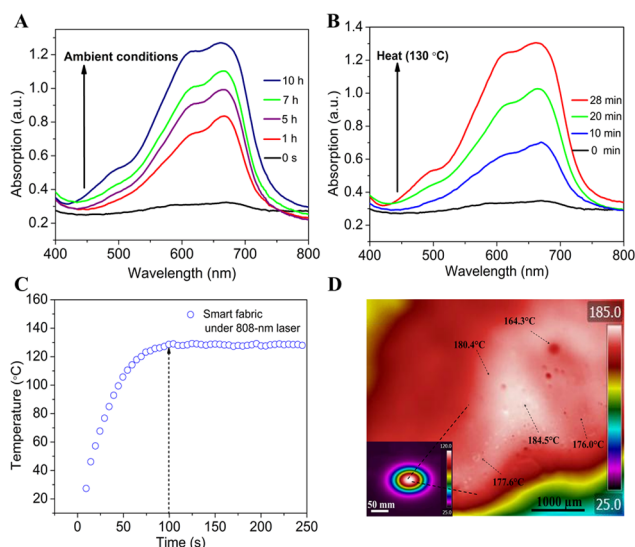
Figure 6. UV−vis−NIR spectra during recoloration process (A) under ambient conditions at room temperature or (B) under direct heating at 130 °C. (C) Temperature changes of the faded smart fabric under the irradiation of 808 nm light ($\sim$1.0 W cm^{-2}) versus time. (D) The corresponding microsurface temperature distribution as monitored by IR camera fitted with a microlens.

unsuitable. To hasten the recoloration process, previous studies have demonstrated that the direct heating of the faded rewritable film/paper at 80−150 °C can enhance the recoloration rate, and the recoloration times are shortened to 30−8 min.[15−17,20,54,55] When the present colorless smart fabric is heated at 130 °C in air, the absorption spectrum goes up gradually with the increased time, and it reverts back to the initial level in 28 min (Figure 6B), which also confirms that heating can shorten the recoloration process. Even so, the required recoloration time ($\sim$28 min) is still too long for the practical application of smart fabric in adaptive camouflage and fashion model wearables. Fortunately, as demonstrated in Figures 3B and S5C,D, the irradiation of NIR light (808 nm, $\sim$1.0 W cm^{-2}) confers the rapid recoloration process in short time, such as 10 s for TiO$_{2-x}$/MB/H$_2$O solution and 100 s for TiO$_{2-x}$/MB/HEC-based smart fabric. It should be noted that when a colorless TiO$_{2-x}$/dye/H$_2$O solution was placed in a cold-water bath (0 °C) and irradiated by 808 nm light ($\sim$1.0 W cm^{-2}), no recoloration could be observed, signifying the importance of localized heat for the rapid recoloration (Figure S7). To study the localized temperature, the colorless smart fabric was illuminated by 808 nm laser, and its temperature was recorded by using a thermographic IR camera. When the 808 nm laser's intensity is $\sim$1.0 W cm^{-2}, the maximal temperature of the irradiated area goes up rapidly from 25 °C (room temperature) at 0 s to 128 °C in 100 s and remains fairly constant upon further irradiation to 250 s (Figure 6C). The NIR-light-induced apparent temperature ($\sim$128 °C) is close to the above uniform heating temperature (130 °C), but the recoloration time (100 s) from NIR light is significantly shorter than that ($\sim$28 min) from uniform heating. To further investigate the reason, infrared camera was fitted with a microlens and the smart fabric irradiated with 808 nm laser under similar conditions to determine the microsurface temperature. Seemingly, when the NIR-light-induced apparent temperature remains at $\sim$128 °C, the microsurface temperature distribution image (Figure 6D) reveals that higher

temperature zones exist on the surface, and they vary from 164.3 to 184.5 °C. This fact reveals the nonuniform temperature distribution from NIR-light irradiation, results from the localized presence of TiO$_{2-x}$ nanorods, which act as photothermal nanoagents. Therefore, NIR-light irradiation can result in the localized high temperature and then rapid recoloration process, which is superior to both recoloration process under ambient air and by conventional uniform heating.[15−17,20,54,55]

Based on the above results, the color-switching mechanism of the smart fabric is proposed as follows (Figure 7). Ti^{3+} self-
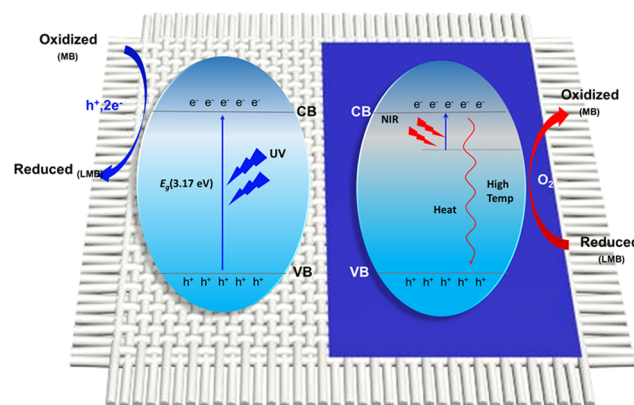
Figure 7. Schematic illustration of color-switching mechanism during the discoloration process by UV-light irradiation and recoloration process by NIR-light irradiation.

doped TiO$_{2-x}$ nanorods have a band gap of $\sim$3.17 eV (Figure S8), which is close to that (3.2 eV) of undoped anatase TiO$_2$. Under the irradiation of UV light (365 nm), TiO$_{2-x}$ nanorods in smart fabric can produce photogenerated holes ($E°$(h$^+$) = +2.91 V) and reductive electrons ($E°$(e$^-$) = −0.32 V) (Figure 7). The oxygen vacancies in TiO$_{2-x}$ nanorods can act as sacrificial electron donors to capture these holes, whereas the remaining electrons reduce blue MB to colorless state LMB ($E°$(MB/LMB) = +0.53 V),[15−17] realizing the rapid discoloration by a photocatalytic reductive process (Figures 3A and 5B). In addition, high concentration of oxygen vacancies confers strong LSPR effect and also enhanced NIR photoabsorption (Figure 2D), and thus TiO$_{2-x}$ nanorods can act as an excellent NIR photothermal nanoagent (Figure 6C,D). Under the irradiation of NIR light (808 nm), TiO$_{2-x}$ nanorods can absorb the light and convert it to heat, resulting in localized high microsurface temperature (164.3−184.5 °C), although the apparent surface temperature is $\sim$128 °C (Figure 6C,D). As previously reported, the recoloration process is governed by the self-catalyzed oxidation of LMB through a process known as photooxidative quenching mechanism:[56] LMB → LMB* and then 2LMB* + O$_2$ = 2MB + 2OH$^-$, where * denotes the electronically excited state. Such a localized high microsurface temperature (164.3−184.5 °C) can accelerate LMB to LMB*, which is better and more rapid than the traditional uniform heating model (80−150 °C). Furthermore, oxygen in air is very important as mentioned above (Figure S5), and it can react with LMB* to produce MB at such high temperatures, realizing the rapid recoloration process (Figures 3B and 5D). Therefore, the present smart fabric exhibits efficient and rapid discoloration process by UV light, as well as
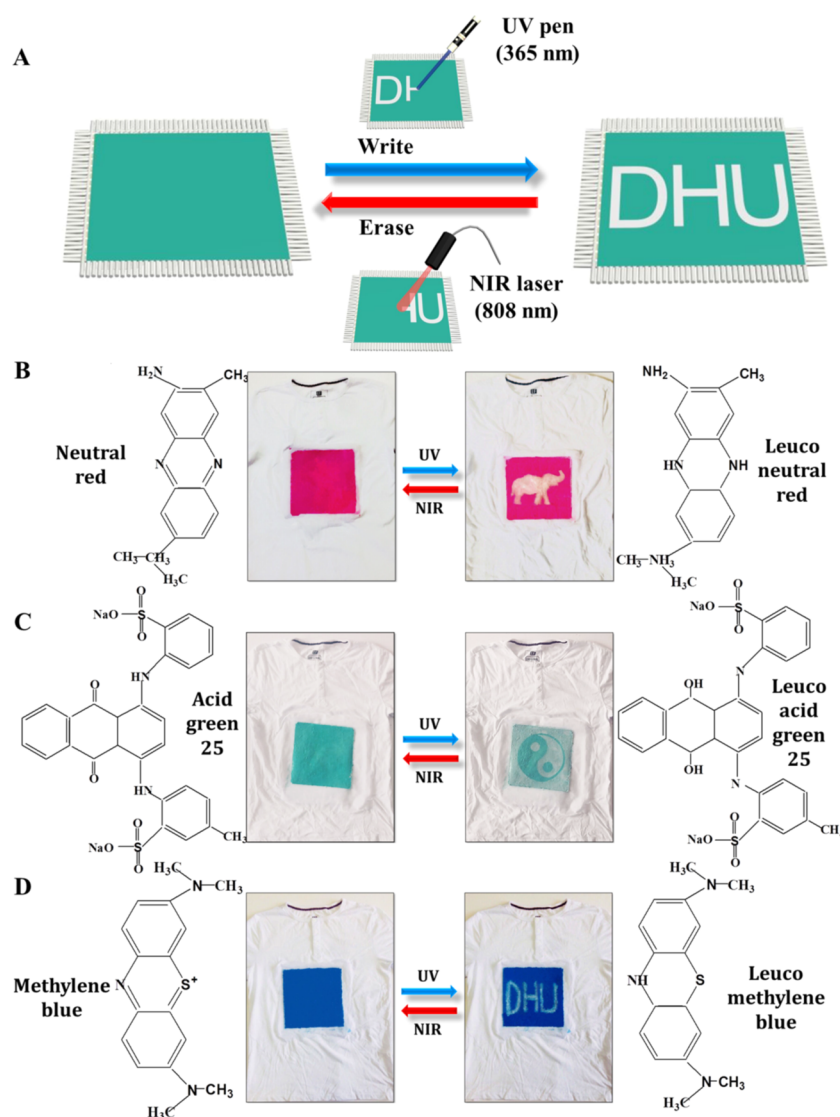
Figure 8. (A) Schematic illustration of writing and erasing process on smart fabric with UV/NIR light. Before and after UV/NIR-light irradiation of rewritable smart T-shirts fabricated using (B) neutral red, (C) acid green 25, and (D) methylene blue as imaging layers.

rapid recoloration process by O_2 and localized high temperature from photothermal effect by NIR light.

It is well known that rewritable smart fabrics may be ideal in meeting the increasing aesthetic or camouflage needs for sensors, information displays, fashion, and security fields. To evaluate their potential in the practical applications, we constructed the smart clothes by coating PDMS and TiO_{2-x}/dye/HEC double layers on the central portions of commercial T-shirts, where dye can be neutral red, acid green 25, or methylene blue for obtaining typical red/green/blue colors. Neutral red is a eurhodin dye with a color index (CI) of 50040, acid green 25 (CI 61570) is a disulfonated anthraquinone derivative, and methylene blue (CI 52015) is a phenothiazine derivative. Under the irradiation of 365 nm UV light (pen or with photomask), the required images and/or letters can be remotely written on the smart T-shirts (Figure 8A), as vividly demonstrated in the video (Supporting Information Video S1). For example, in red (Figure 8B), green (Figure 8C), or blue (Figure 8D) central portions of T-shirts, the irradiated region turns white due to the change from colored dye to the colorless leuco form, whereas the unirradiated regions retain the original

color of dye, resulting in the appearance of animal shape, Tai-Chi symbol, and letters with high resolution. Under the irradiation of 808 nm light, the images and/or letters can be erased from T-shirts (Figure 8A), as clearly shown in the video (Supporting Information Video S2). For example, the printed images and letters completely vanished and their colors reverted to the original dye color, resulting from the evolution from colorless leuco form to colored dye (Figure 8B−D). These results demonstrate the successful fabrication of smart clothes, which can be remotely printed by UV light and then rapidly erased by NIR light.

For the practical application of such rewritable smart clothes, one prerequisite is the good reversibility and stability. To evaluate the cycle stability, the smart fabric was illuminated with UV light and then NIR light repeatedly in the writing/erasing process, and its absorption spectra were real-time recorded. The graph was plotted by using the absorption maxima and minima of the smart fabric after UV/NIR irradiation (Figure 9). In each cycle (during the entire 23 cycles), the photoabsorption intensity goes down to 0.3 after UV-light irradiation for 180−240 s. There is no obvious
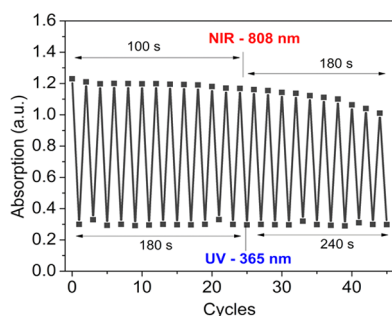
Figure 9. Absorption intensity of the smart fabric recorded at approximately 668 nm under alternating UV- and NIR-light irradiation for 23 cycles.

change in the absorption minima, indicating that smart fabric has good stability during the UV-light-induced discoloration process. After NIR-light irradiation for 100 s in the first 13 cycles, the photoabsorption maxima goes up to ~1.2, also demonstrating excellent stability. During these cycles, the smart fabric does not show any physical changes and no appearance of cracks or aggregations. With the further increase of the cycles from 13 to 23, there is a slight decay in the photoabsorption maxima due to the exhaustion of oxygen vacancies acting as SEDs, which has been revealed in previous report.[15] Thus, the fabric required longer exposure time of UV (240 s) and NIR (180 s) light for the discoloration and recoloration cycles, respectively. It should be pointed out that this decay can be avoided or weakened by resting the fabric overnight, increasing TiO_{2-x} nanorods concentration, or extending the irradiation time. In addition, the smart fabric shows no obvious color changes after the exposure to simulated natural light (one sun, 1 kW m^{-2}) for 20 min (Figure S9) and after being stored for more than 6 months (Figure S10), indicating excellent stability. Furthermore, the smart fabric also shows excellent color fastness after it has been washed in water (Figure S11, Supporting Information Video S3) and rubbed with a glass rod (Figure S12), since the hydrogen bonding between the abundant −OH groups on HEC molecules and chemical groups of dyes (such as −N(CH₃)₂ groups in MB and LMB) can fix the dye molecule on the surface of the fabric.[15] Therefore, these rewritable smart fabrics have good reversibility and stability.

4. CONCLUSIONS

Ti^{3+} self-doped TiO_{2-x} nanorods have been prepared, and they have oxygen vacancies in the bulk, strong UV (band gap: ~3.17 eV) and NIR photoabsorption. TiO_{2-x}/dye/HEC-based PCSS has been used to construct smart fabric. Under the irradiation of UV light, various red/green/blue figures or letters can be rapidly and remotely printed on fabrics in 180 s due to the efficient photocatalytic reduction of the redox dye. Under the irradiation of NIR light, figures or letters on a fabric can be erased in a very short time (~100 s, far lower than 28 min from traditional uniform heating method at 130 °C), resulting from the rapid recoloration process by the efficient oxidization due to the localized high temperature in air (O₂). Therefore, the present rewritable smart fabric is a great advancement with great potential in the practical applications in aesthetic clothes for adaptive camouflage in sensors, information displays, fashion/aesthetic, and security fields.

■ ASSOCIATED CONTENT

ⓢ Supporting Information

The Supporting Information is available free of charge on the ACS Publications website at DOI: 10.1021/acsami.8b22443.

> Characterization details, TEM image of undoped TiO_2 nanorods, EDS patterns and further XPS spectrum of TiO_{2-x} and TiO_2 samples, hydrophobicity experiment, effect of oxygen in NIR-based recoloration of smart fabric, effect of heat on recoloration in PCSS solution, band gap determination, effects of light/storage/washing/rubbing on the color fastness (PDF)

> Writing with UV light pen (365 nm) (AVI)

> Erasing with 808 nm laser (AVI)

> Washing fastness test (AVI)

■ AUTHOR INFORMATION

Corresponding Authors

*Email: zgchen@dhu.edu.cn. Tel: +86-21-67792975. Fax: +86-21-67792855 (Z.C.).

*Email: zhumf@dhu.edu.cn. Tel: +86-21-67792849. Fax: +86-21-67792855 (M.Z.).

ORCID ⓘ

Zhigang Chen: 0000-0003-3676-6019

Meifang Zhu: 0000-0003-0359-3633

Notes

The authors declare no competing financial interest.

■ ABBREVIATIONS

PCSS, photoreversible color-switching systems
HEC, hydroxyethyl cellulose
SED, sacrificial electron donor
NIR, near infrared
MB, methylene blue
NR, neutral red
AG, acid green 25
PDMS, poly(dimethylsiloxane)

■ REFERENCES

(1) Sato, O. Dynamic Molecular Crystals with Switchable Physical Properties. *Nat. Chem.* **2016**, *8*, 644−656.

(2) Kundu, P. K.; Samanta, D.; Leizrowice, R.; Margulis, B.; Zhao, H.; Börner, M.; Udayabhaskararao, T.; Manna, D.; Klajn, R. Light-Controlled Self-Assembly of Non-Photoresponsive Nanoparticles. *Nat. Chem.* **2015**, *7*, 646−652.

(3) Ohko, Y.; Tatsuma, T.; Fujii, T.; Naoi, K.; Niwa, C.; Kubota, Y.; Fujishima, A. Multicolour Photochromism of TiO₂ Films Loaded with Silver Nanoparticles. *Nat. Mater.* 2003, 2, 29−31.

(4) Klajn, R.; Wesson, P. J.; Bishop, K. J.; Grzybowski, B. A. Writing Self-Erasing Images Using Metastable Nanoparticle "Inks". *Angew. Chem., Int. Ed.* 2009, 48, 7035−7039.

(5) Jeong, W.; Khazi, M. I.; Park, D.-H.; Jung, Y.-S.; Kim, J.-M. Full Color Light Responsive Diarylethene Inks for Reusable Paper. *Adv. Funct. Mater.* 2016, 26, 5230−5238.

(6) Russew, M.-M.; Hecht, S. Photoswitches: From Molecules to Materials. *Adv. Mater.* 2010, 22, 3348−3360.

(7) Iqbal, K. M.; Woomin, J.; Jong-Man, K. Functional Materials and Systems for Rewritable Paper. *Adv. Mater.* 2018, 30, No. 1705310.

(8) Yang, Y.; Hughes, R. P.; Aprahamian, I. Near-Infrared Light Activated Azo-BF2 Switches. *J. Am. Chem. Soc.* 2014, 136, 13190−13193.

(9) Samanta, D.; Gemen, J.; Chu, Z.; Diskin-Posner, Y.; Shimon, L. J. W.; Klajn, R. Reversible Photoswitching of Encapsulated Azobenzenes In Water. *Proc. Natl. Acad. Sci. U.S.A.* 2018, 115, 9379−9384.

(10) Samanta, D.; Galaktionova, D.; Gemen, J.; Shimon, L. J. W.; Diskin-Posner, Y.; Avram, L.; Král, P.; Klajn, R. Reversible Chromism of Spiropyran in the Cavity of A Flexible Coordination Cage. *Nat. Commun.* 2018, 9, No. 641.

(11) Baroncini, M.; d'Agostino, S.; Bergamini, G.; Ceroni, P.; Comotti, A.; Sozzani, P.; Bassanetti, I.; Grepioni, F.; Hernandez, T. M.; Silvi, S.; Venturi, M.; Credi, A. Photoinduced Reversible Switching of Porosity In Molecular Crystals Based on Star-Shaped Azobenzene Tetramers. *Nat. Chem.* 2015, 7, 634−640.

(12) Qin, T.; Han, J.; Geng, Y.; Ju, L.; Sheng, L.; Zhang, S. X.-A. A Multiaddressable Dyad with Switchable Cyan/Magenta/Yellow Colors for Full-Color Rewritable Paper. *Chem. - Eur. J.* 2018, 24, 12539−12545.

(13) Hemmer, J. R.; Poelma, S. O.; Treat, N.; Page, Z. A.; Dolinski, N. D.; Diaz, Y. J.; Tomlinson, W.; Clark, K. D.; Hooper, J. P.; Hawker, C.; Read de Alaniz, J. Tunable Visible and Near Infrared Photoswitches. *J. Am. Chem. Soc.* 2016, 138, 13960−13966.

(14) Helmy, S.; Leibfarth, F. A.; Oh, S.; Poelma, J. E.; Hawker, C. J.; Read de Alaniz, J. Photoswitching Using Visible Light: A New Class of Organic Photochromic Molecules. *J. Am. Chem. Soc.* 2014, 136, 8169−8172.

(15) Wang, W.; Xie, N.; He, L.; Yin, Y. Photocatalytic Colour Switching of Redox Dyes For Ink-Free Light-Printable Rewritable Paper. *Nat. Commun.* 2014, 5, No. 5459.

(16) Wang, W.; Ye, Y.; Feng, J.; Chi, M.; Guo, J.; Yin, Y. Enhanced Photoreversible Color Switching of Redox Dyes Catalyzed by Barium-Doped TiO₂ Nanocrystals. *Angew. Chem., Int. Ed.* 2015, 54, 1321−1326.

(17) Wang, W.; Feng, J.; Ye, Y.; Lyu, F.; Liu, Y.-s.; Guo, J.; Yin, Y. Photocatalytic Color Switching of Transition Metal Hexacyanometalate Nanoparticles for High-Performance Light-Printable Rewritable Paper. *Nano Lett.* 2017, 17, 755−761.

(18) Wang, W.; Liu, L.; Feng, J.; Yin, Y. Photocatalytic Reversible Color Switching Based on Titania Nanoparticles. *Small Methods* 2018, 2, No. 1700273.

(19) Lee, S.-K.; Sheridan, M.; Mills, A. Novel UV-Activated Colorimetric Oxygen Indicator. *Chem. Mater.* 2005, 17, 2744−2751.

(20) Han, D.; Jiang, B.; Feng, J.; Yin, Y.; Wang, W. Photocatalytic Self-Doped SnO₂₋ₓ Nanocrystals Drive Visible-Light-Responsive Color Switching. *Angew. Chem., Int. Ed.* 2017, 56, 7792−7796.

(21) Wang, W.; Ye, M.; He, L.; Yin, Y. Nanocrystalline TiO₂-Catalyzed Photoreversible Color Switching. *Nano Lett.* 2014, 14, 1681−1686.

(22) Mills, A.; Hazafy, D. Nanocrystalline SnO₂-based, UVB-activated, Colourimetric Oxygen Indicator. *Sens. Actuators, B* 2009, 136, 344−349.

(23) Lawrie, K.; Mills, A.; Hazafy, D. Simple Inkjet-Printed, UV-Activated Oxygen Indicator. *Sens. Actuators, B* 2013, 176, 1154−1159.

(24) Zhang, Z.; Guo, K.; Li, Y.; Li, X.; Guan, G.; Li, H.; Luo, Y.; Zhao, F.; Zhang, Q.; Wei, B.; Pei, Q.; Peng, H. A Colour-Tunable, Weavable Fibre-Shaped Polymer Light-Emitting Electrochemical Cell. *Nat. Photonics* 2015, 9, No. 233.

(25) Won, R. Colour-Tunable Textiles. *Nat. Photonics* 2008, 2, No. 650.

(26) Graham-Rowe, D. Photonic Fabrics Take Shape. *Nat. Photonics* 2007, 1, No. 6.

(27) Yoon, J.; Jeong, Y.; Kim, H.; Yoo, S.; Jung, H. S.; Kim, Y.; Hwang, Y.; Hyun, Y.; Hong, W.-K.; Lee, B. H.; Choa, S.-H.; Ko, H. C. Robust and Stretchable Indium Gallium Zinc Oxide-Based Electronic Textiles Formed by Cilia-Assisted Transfer Printing. *Nat. Commun.* 2016, 7, No. 11477.

(28) Stoppa, M.; Chiolerio, A. Wearable Electronics and Smart Textiles: A Critical Review. *Sensors* 2014, 14, 11957−11992.

(29) Krogman, K. C.; Lowery, J. L.; Zacharia, N. S.; Rutledge, G. C.; Hammond, P. T. Spraying asymmetry into functional membranes layer-by-layer. *Nat. Mater.* 2009, 8, No. 512.

(30) Son, D.; Kang, J.; Vardoulis, O.; Kim, Y.; Matsuhisa, N.; Oh, J. Y.; To, J. W. F.; Mun, J.; Katsumata, T.; Liu, Y.; McGuire, A. F.; Krason, M.; Molina-Lopez, F.; Ham, J.; Kraft, U.; Lee, Y.; Yun, Y.; Tok, J. B. H.; Bao, Z. An Integrated Self-Healable Electronic Skin System Fabricated Via Dynamic Reconstruction of a Nanostructured Conducting Network. *Nat. Nanotechnol.* 2018, 13, 1057−1065.

(31) Wang, S.; Xu, J.; Wang, W.; Wang, G.-J. N.; Rastak, R.; Molina-Lopez, F.; Chung, J. W.; Niu, S.; Feig, V. R.; Lopez, J.; Lei, T.; Kwon, S.-K.; Kim, Y.; Foudeh, A. M.; Ehrlich, A.; Gasperini, A.; Yun, Y.; Murmann, B.; Tok, J. B. H.; Bao, Z. Skin Electronics from Scalable Fabrication of an Intrinsically Stretchable Transistor Array. *Nature* 2018, 555, No. 83.

(32) Pinto, T. V.; Costa, P.; Sousa, C. M.; Sousa, C. A. D.; Pereira, C.; Silva, C. J. S. M.; Pereira, M. F. R.; Coelho, P. J.; Freire, C. Screen-Printed Photochromic Textiles through New Inks Based on SiO₂@ naphthopyran Nanoparticles. *ACS Appl. Mater. Interfaces* 2016, 8, 28935−28945.

(33) Kinashi, K.; Iwata, T.; Tsuchida, H.; Sakai, W.; Tsutsumi, N. Composite Resin Dosimeters: A New Concept and Design for a Fibrous Color Dosimeter. *ACS Appl. Mater. Interfaces* 2018, 10, 11926−11932.

(34) Cao, D.; Xu, C.; Lu, W.; Qin, C.; Cheng, S. Sunlight-Driven Photo-Thermochromic Smart Windows. *Sol. RRL* 2018, 2, No. 1700219.

(35) Gelebart, A. H.; Vantomme, G.; Meijer, E. W.; Broer, D. J. Mastering the Photothermal Effect in Liquid Crystal Networks: A General Approach for Self-Sustained Mechanical Oscillators. *Adv. Mater.* 2017, 29, No. 1606712.

(36) Fang, C.; Shao, L.; Zhao, Y.; Wang, J.; Wu, H. A Gold Nanocrystal/Poly(dimethylsiloxane) Composite for Plasmonic Heating on Microfluidic Chips. *Adv. Mater.* 2012, 24, 94−98.

(37) Chen, H.; Zhang, W.; Zhu, G.; Xie, J.; Chen, X. Rethinking Cancer Nanotheranostics. *Nat. Rev. Mater.* 2017, 2, No. 17024.

(38) Shi, J.; Kantoff, P. W.; Wooster, R.; Farokhzad, O. C. Cancer Nanomedicine: Progress, Challenges and Opportunities. *Nat. Rev. Cancer* 2017, 17, 20−27.

(39) Tian, Q.; Tang, M.; Sun, Y.; Zou, R.; Chen, Z.; Zhu, M.; Yang, S.; Wang, J.; Wang, J.; Hu, J. Hydrophilic Flower-Like CuS Superstructures as an Efficient 980 nm Laser-Driven Photothermal Agent for Ablation of Cancer Cells. *Adv. Mater.* 2011, 23, 3542−3547.

(40) Tian, Q.; Jiang, F.; Zou, R.; Liu, Q.; Chen, Z.; Zhu, M.; Yang, S.; Wang, J.; Wang, J.; Hu, J. Hydrophilic Cu₉S₅ Nanocrystals: A Photothermal Agent with a 25.7% Heat Conversion Efficiency for Photothermal Ablation of Cancer Cells in Vivo. *ACS Nano* 2011, 5, 9761−9771.

(41) Chen, Z.; Wang, Q.; Wang, H.; Zhang, L.; Song, G.; Song, L.; Hu, J.; Wang, H.; Liu, J.; Zhu, M.; Zhao, D. Ultrathin PEGylated W₁₈O₄₉ Nanowires as a New 980 nm-Laser-Driven Photothermal Agent for Efficient Ablation of Cancer Cells In Vivo. *Adv. Mater.* 2013, 25, 2095−2100.

(42) Yu, N.; Hu, Y.; Wang, X.; Liu, G.; Wang, Z.; Liu, Z.; Tian, Q.; Zhu, M.; Shi, X.; Chen, Z. Dynamically Tuning Near-Infrared-Induced Photothermal Performances of TiO_2 Nanocrystals By Nb Doping For Imaging-Guided Photothermal Therapy of Tumors. *Nanoscale* **2017**, *9*, 9148−9159.

(43) Li, F.; Hou, H.; Yin, J.; Jiang, X. Near-Infrared Light−Responsive Dynamic Wrinkle Patterns. *Sci. Adv.* **2018**, *4*, No. eaar5762.

(44) Cherrington, M.; Claypole, T. C.; Deganello, D.; Mabbett, I.; Watson, T.; Worsley, D. Ultrafast Near-Infrared Sintering of a Slot-Die Coated Nano-Silver Conducting Ink. *J. Mater. Chem.* **2011**, *21*, 7562−7564.

(45) Zhu, Q.; Peng, Y.; Lin, L.; Fan, C.-M.; Gao, G.-Q.; Wang, R.-X.; Xu, A.-W. Stable Blue TiO_{2-x} Nanoparticles For Efficient Visible Light Photocatalysts. *J. Mater. Chem. A* **2014**, *2*, 4429−4437.

(46) Tian, F.; Zhang, Y.; Zhang, J.; Pan, C. Raman Spectroscopy: A New Approach to Measure the Percentage of Anatase TiO_2 Exposed (001) Facets. *J. Phys. Chem. C* **2012**, *116*, 7515−7519.

(47) Chen, X.; Liu, L.; Yu, P. Y.; Mao, S. S. Increasing Solar Absorption for Photocatalysis with Black Hydrogenated Titanium Dioxide Nanocrystals. *Science* **2011**, *331*, 746−750.

(48) Han, E.; Vijayarangamuthu, K.; Youn, J.-s.; Park, Y.-K.; Jung, S.-C.; Jeon, K.-J. Degussa P25 TiO_2 modified with H_2O_2 under microwave treatment to enhance photocatalytic properties. *Catal. Today* **2018**, *303*, 305−312.

(49) Kumar, R.; Govindarajan, S.; Siri Kiran Janardhana, R. K.; Rao, T. N.; Joshi, S. V.; Anandan, S. Facile One-Step Route for the Development of in Situ Cocatalyst-Modified Ti^{3+} Self-Doped TiO_2 for Improved Visible-Light Photocatalytic Activity. *ACS Appl. Mater. Interfaces* **2016**, *8*, 27642−27653.

(50) Xing, M.; Fang, W.; Nasir, M.; Ma, Y.; Zhang, J.; Anpo, M. Self-Doped Ti^{3+}-Enhanced TiO_2 Nanoparticles with a High-Performance Photocatalysis. *J. Catal.* **2013**, *297*, 236−243.

(51) Imran, M.; Yousaf, A. B.; Zhou, X.; Liang, K.; Jiang, Y.-F.; Xu, A.-W. Oxygen-Deficient TiO_{2-x}/Methylene Blue Colloids: Highly Efficient Photoreversible Intelligent Ink. *Langmuir* **2016**, *32*, 8980−8987.

(52) Sasan, K.; Zuo, F.; Wang, Y.; Feng, P. Self-Doped Ti^{3+}-TiO_2 as a Photocatalyst for the Reduction of CO_2 Into a Hydrocarbon Fuel Under Visible Light Irradiation. *Nanoscale* **2015**, *7*, 13369−13372.

(53) Zuo, F.; Wang, L.; Wu, T.; Zhang, Z.; Borchardt, D.; Feng, P. Self-Doped Ti^{3+} Enhanced Photocatalyst for Hydrogen Production under Visible Light. *J. Am. Chem. Soc.* **2010**, *132*, 11856−11857.

(54) Evans, R. A.; Hanley, T. L.; Skidmore, M. A.; Davis, T. P.; Such, G. K.; Yee, L. H.; Ball, G. E.; Lewis, D. A. The Generic Enhancement of Photochromic Dye Switching Speeds In A Rigid Polymer Matrix. *Nat. Mater.* **2005**, *4*, 249−253.

(55) Zhang, T.; Sheng, L.; Liu, J.; Ju, L.; Li, J.; Du, Z.; Zhang, W.; Li, M.; Zhang, S. X.-A. Photoinduced Proton Transfer between Photoacid and pH-Sensitive Dyes: Influence Factors and Application for Visible-Light-Responsive Rewritable Paper. *Adv. Funct. Mater.* **2018**, *28*, No. 1705532.

(56) Lee, S.-K.; Mills, A. Novel photochemistry of leuco-Methylene Blue. *Chem. Commun.* **2003**, 2366−2367.